Weak ferromagnetism and other instabilities of the two-dimensional t-t' Hubbard model at van Hove fillings

V. Hankevych,[1,2] B. Kyung,[1] and A.-M. S. Tremblay[1,3]
[1]*Département de physique and Regroupement québécois sur les matériaux de pointe, Université de Sherbrooke, Sherbrooke, Québec, Canada J1K 2R1*
[2]*Department of Physics, Ternopil State Technical University, 56 Rus'ka St., UA-46001 Ternopil, Ukraine*
[3]*Institut canadien de recherches avancées, Université de Sherbrooke, Sherbrooke, Québec, Canada J1K 2R1*
(Received 11 June 2003; revised manuscript received 12 September 2003; published 5 December 2003)

We investigate magnetic and superconducting instabilities of the two-dimensional t-t' Hubbard model on a square lattice at van Hove densities from weak to intermediate coupling by means of the two-particle self-consistent approach. We find that as the next-nearest-neighbor hopping $|t'|$ increases from zero, the leading instability is towards an incommensurate spin-density wave whose wave vector moves slowly away from (π,π). For intermediate values of $|t'|$, the leading instability is towards $d_{x^2-y^2}$-wave superconductivity. For larger $|t'|>0.33t$, there are signs of a crossover to ferromagnetism at extremely low temperatures. The suppression of the crossover temperature is driven by Kanamori screening that strongly renormalizes the effective interaction and also causes the crossover temperature to depend only weakly on t'. Electronic self-energy effects for large $|t'|$ lead to considerable reduction of the zero-energy single-particle spectral weight beginning at temperatures as high as $T\lesssim 0.1t$, an effect that may be detrimental to the existence of a ferromagnetic ground state at weak coupling.

DOI: 10.1103/PhysRevB.68.214405 PACS number(s): 75.10.Lp, 71.10.Fd, 71.27.+a

I. INTRODUCTION

Historically, the single-band Hubbard model was suggested independently by Gutzwiller,[1] Hubbard,[2] and Kanamori[3] to gain insight into the origin of metallic ferromagnetism. However, despite enormous efforts[4] that were undertaken to find answers to this question, only a few reliable results have been obtained even for this simplest possible microscopic model. The Hubbard model also exhibits a variety of other competing phases, including antiferromagnetic and superconducting phases.

The first exact results for ferromagnetism were obtained in the strong-coupling limit, $U\to\infty$, by Nagaoka[5] and Thouless[6] who showed that the ground state of the Hubbard model with one hole or electron is ferromagnetic at an infinitely large Coulomb repulsion. That result did not answer the question of stability to a finite concentration of holes in the thermodynamic limit. Improved bounds for the Nagaoka state have recently been derived[7] for various lattices in two and three dimensions. Ferromagnetic ground states also occur if one of the several bands of the model is dispersionless (so-called Lieb's ferrimagnetism[8] and flat-band ferromagnetism[9]). Mielke and Tasaki proved the local stability of ferromagnetic ground states in the Hubbard model with nearly flat[10] and partially filled[11] bands. Reference 12 contains a short review of these works as well as new results for Hubbard models without the singularities associated with flat bands. A review of results[13] obtained for the simple one-band Hubbard model in the last few years as well as the results of Mielke and Tasaki suggest that the important ingredients for ferromagnetism in that model are (a) an interaction strength that is in the intermediate to strong coupling regime and (b) a band that exhibits a strong asymmetry and a large density of states near the Fermi energy or near one of the band edges. Metallic ferromagnetism at weak coupling, usually known as Stoner ferromagnetism, has in fact been ruled out a long time ago by Kanamori[3] based on the argument that the renormalization of the interaction strength brought about by T-matrix effects (Kanamori screening) would never allow the Stoner criterion to be satisfied when the density of states at the Fermi level $\rho(E_F)$ is nonsingular. Physically, the largest possible effective interaction, according to Kanamori, is equal to the kinetic-energy cost for making the two-particle wave function vanish when the two particles are at the same site. That energy scales like the bandwidth $\rho(E_F)^{-1}$ so that the Stoner criterion $1-U\rho(E_F)=0$ cannot be fulfilled. Quantum Monte Carlo calculations confirm the quantitative nature of Kanamori's T-matrix result.[14]

If there is Stoner-type ferromagnetism in weak to intermediate coupling, it is thus clear that, as in the moderate to strong-coupling case, one needs at least a singular density of states to overcome Kanamori screening. An example of a model with singular density of states at the Fermi energy as well as band asymmetry is the two-dimensional (2D) Hubbard model with both nearest neighbor t and next-nearest-neighbor t' hoppings. When the Fermi energy is close to the van Hove singularity the corresponding filling is usually referred to as a ''van Hove filling.'' At that filling, the Fermi surface passes through the saddle points of the single-particle dispersion. There are, however, other phases competing with ferromagnetism. At weak to moderate values of the on-site Coulomb repulsion U, for small t'/t and close to half-filling, the 2D t-t' Hubbard model shows an antiferromagnetic instability. That instability due to nesting is however destroyed[15] for a sufficiently large ratio t'/t at weak interactions in two and three dimensions, thus leaving room for other instabilities, including d-wave superconductivity and metallic ferromagnetism.

The questions that we address in this paper are thus the following. Can the asymmetry of the band and the large density of states near the Fermi energy overcome the Kanamori argument and lead to ferromagnetism in the 2D Hubbard model? What are the competing phases? Most results on this problem (particularly for a square lattice) fall into three different classes.

(a) Momentum-cutoff renormalization-group (RG) methods[16,17] and quantum Monte Carlo calculations[18] suggest that there is no evidence for ferromagnetism. But the problem, in particular with numerical methods, is that only very small system sizes can be used in a regime where the size dependence is important. In addition, momentum-cutoff RG does not allow the contribution of ferromagnetic fluctuations.[19] So these results should not be considered conclusive.

(b) The second class of results is based on Wegner's flow equations. They show[20] a tendency towards weak ferromagnetism with s^*-wave character (the order parameter changes sign close to the Fermi energy). According to the flow equations calculations this phase competes with other instabilities in the particle-hole channel, in particular with the Pomeranchuk instability. The difficulty of those weak-coupling calculations is that the s^*-magnetic phase occurs at stronger coupling than the regime of validity of the second-order analysis in U of the flow equations.

(c) The third class suggests clear evidence for ferromagnetic ground states. These works include a projector quantum Monte Carlo calculation with 20×20 sites and the T-matrix technique,[21] a generalized random-phase approximation (RPA) including particle-particle scattering[22] and exact diagonalizations.[23] Similar tendencies have been found by the authors of Refs. 24 and 25 within the renormalization-group and parquet approaches for the so-called two-patch model. Honerkamp and Salmhofer recently studied[19] the stability of this ferromagnetic region at finite temperatures by means of a temperature-cutoff renormalization-group (TCRG) technique analogous to that used earlier for one-dimensional systems.[26] For $U=3$, they have found that the ferromagnetic instability is the leading one for $|t'|>0.33|t|$ at van Hove fillings with the critical temperature strongly dependent on the value of t'. When the electron concentration deviates slightly away from the van Hove filling, the tendency towards ferromagnetism is cut off at low temperatures and a triplet p-wave superconducting phase dominates. The U dependence of these ferromagnetic and superconducting phases in the ground state has been studied in Ref. 27 by means of the same TCRG at weak coupling.

In the present paper we study ferromagnetism and competing phases in the t-t' Hubbard model at weak to intermediate couplings by means of the two-particle self-consistent (TPSC) approach.[28] Antiferromagnetism and $d_{x^2-y^2}$-wave superconductivity are the competing instabilities. The TPSC approach is nonperturbative and applies up to intermediate coupling. It enforces the Pauli principle, conservation laws, and includes the Kanamori screening effect. Comparisons with quantum Monte Carlo calculations have shown that TPSC is the analytical approach that gives the most accurate results for the spin structure factor,[29] the spin susceptibility,[28] and the $d_{x^2-y^2}$-wave susceptibility[30] in two dimensions. Throughout the paper we consider the 2D t-t' Hubbard model at van Hove fillings from weak to moderate couplings. We determine the regions of the T-t' plane where the uniform paramagnetic phase becomes unstable to various types of fluctuations. We also estimate the electronic self-energy effects for large t' where ferromagnetic effects are present. The following section recalls the methodology. We then present the results and conclude.

II. TWO-PARTICLE SELF-CONSISTENT APPROACH

We consider the t-t' Hubbard model on a square lattice with nearest (t) and next-nearest (t') neighbor hoppings

$$H=-t\sum_{\langle ij\rangle\sigma}(c^{\dagger}_{i\sigma}c_{j\sigma}+\text{H.c.})-t'\sum_{\langle\langle ij\rangle\rangle\sigma}(c^{\dagger}_{i\sigma}c_{j\sigma}+\text{H.c.})+U\sum_{i}n_{i\uparrow}n_{i\downarrow}, \tag{1}$$

where $c^{\dagger}_{i\sigma}$ ($c_{i\sigma}$) is the creation (annihilation) operator for the electrons with spin projection $\sigma\in\{\uparrow,\downarrow\}$, U is the local Coulomb repulsion for two electrons of opposite spins on the same site, and $n_{i\sigma}=c^{\dagger}_{i\sigma}c_{i\sigma}$ is the occupation number. The bare single-particle dispersion has the form, in units where lattice spacing is unity,

$$\varepsilon_{\mathbf{k}}=-2t(\cos k_x+\cos k_y)-4t'\cos k_x\cos k_y. \tag{2}$$

This spectrum leads to a van Hove singularity in the density of states coming from saddle points of the dispersion relation that are located at $\mathbf{k}=(0,\pm\pi)$ and $(\pm\pi,0)$. The corresponding energy is $\varepsilon_{VH}=4t'$. In this paper we always consider the case where the noninteracting chemical potential is $4t'$, so that the noninteracting Fermi surface crosses the saddle points and the noninteracting density of states diverges logarithmically at the Fermi energy. The filling corresponding to this choice of chemical potential is a ''van Hove filling.'' For $t'=0$ and half-filling the Fermi surface is perfectly nested, namely, $\varepsilon_{\mathbf{k}+\mathbf{Q}}=-\varepsilon_{\mathbf{k}}$, with $\mathbf{Q}=(\pi,\pi)$, which leads to an antiferromagnetic instability for $U>0$. The perfect nesting is removed for $t'/t\neq 0$. We work in units where Bolzmann's constant k_B and nearest-neighbor hopping t are all unity.

The TPSC approach[28] can be summarized as follows.[31] We use the functional method of Schwinger-Martin-Kadanoff-Baym with source field ϕ to first generate exact equations for the self-energy Σ and response (four-point) functions for spin and charge excitations (spin-spin and density-density correlation functions). In such a scheme, spin and charge dynamical susceptibilities can be obtained from the functional derivatives of the source-dependent propagator G with respect to ϕ. Our nonperturbative approach then consists in two steps.

At the first level of approximation, we use the following two-particle self-consistent scheme to determine the two-particle quantities: We apply a Hartree-Fock-type factorization of the four-point response function that defines the product ΣG, but we also impose the important additional constraint that the factorization is exact when all space-time

coordinates of the four-point function coincide. From the corresponding self-energy, we obtain the local momentum- and frequency-independent irreducible particle-hole vertex appropriate for the spin response

$$U_{sp}=\frac{\delta\Sigma_{\uparrow}}{\delta G_{\downarrow}}-\frac{\delta\Sigma_{\uparrow}}{\delta G_{\uparrow}}=U\frac{\langle n_{\uparrow}n_{\downarrow}\rangle}{\langle n_{\uparrow}\rangle\langle n_{\downarrow}\rangle}. \tag{3}$$

The renormalization of this vertex mainly comes[14,28] from Kanamori screening.[3] The double occupancy $\langle n_{\uparrow}n_{\downarrow}\rangle$ entering this equation is then obtained self-consistently using the fluctuation-dissipation theorem and the Pauli principle. More specifically, the Pauli principle $\langle n_{\sigma}^2\rangle=\langle n_{\sigma}\rangle$ implies that

$$\langle(n_{\uparrow}-n_{\downarrow})^2\rangle=\langle n_{\uparrow}\rangle+\langle n_{\downarrow}\rangle-2\langle n_{\uparrow}n_{\downarrow}\rangle,$$

while the fluctuation-dissipation theorem leads to an equality between the equal-time equal-position correlation $\langle(n_{\uparrow}-n_{\downarrow})^2\rangle$ and the corresponding susceptibility, namely,

$$\langle(n_{\uparrow}-n_{\downarrow})^2\rangle=\frac{T}{N}\sum_{q}\chi_{sp}^{(1)}(q)=n-2\langle n_{\uparrow}n_{\downarrow}\rangle, \tag{4}$$

where, using the shorthand $q\equiv(\mathbf{q},2i\pi mT)$, the summation is over all wave vectors and all Matsubara frequencies with T being the temperature, n being the electron filling, and N being the number of lattice sites. The latter equation is a self-consistent equation for the double occupancy, or equivalently for U_{sp} in Eq. (3), because the spin susceptibility entering the above equation is

$$\chi_{sp}^{(1)}(q)=\frac{\chi_0(q)}{1-\frac{1}{2}U_{sp}\chi_0(q)}, \tag{5}$$

where $\chi_0(q)$ is the particle-hole irreducible susceptibility including the contribution from both spin components,

$$\chi_0(q)=\frac{2}{N}\sum_{\mathbf{k}}\frac{f(\varepsilon_{\mathbf{k}})-f(\varepsilon_{\mathbf{k}+\mathbf{q}})}{2i\pi mT-\varepsilon_{\mathbf{k}}+\varepsilon_{\mathbf{k}+\mathbf{q}}}, \tag{6}$$

with $f(\varepsilon)$ being the Fermi-Dirac distribution function. Equation (4) is also known as the local-moment sum rule. The Green functions at this first level of approximation, $G^{(1)}$, contain a self-energy $\Sigma^{(1)}$ that depends on double occupancy; but, since this self-energy is momentum and frequency independent, it can be absorbed in the definition of the chemical potential. In the above then, $G^{(1)}$ is the bare propagator and χ_0 is the bare particle-hole susceptibility both evaluated with the noninteracting chemical potential μ_0 corresponding to the desired filling. The irreducible charge vertex $U_{ch}=\delta\Sigma_{\uparrow}/\delta G_{\downarrow}+\delta\Sigma_{\uparrow}/\delta G_{\uparrow}$ strictly speaking is not momentum and frequency independent. Nevertheless, assuming for simplicity that it is, it can be simply found by using the fluctuation-dissipation theorem for charge fluctuations and the Pauli principle,

$$\frac{T}{N}\sum_{q}\chi_{ch}^{(1)}(q)=n+2\langle n_{\uparrow}n_{\downarrow}\rangle-n^2,$$

with

$$\chi_{ch}^{(1)}(q)=\frac{\chi_0(q)}{1+\frac{1}{2}U_{ch}\chi_0(q)}. \tag{7}$$

The spin and charge susceptibilities obtained from Eqs. (5) and (7) satisfy conservation laws.[28,29] This approach, which satisfies the Pauli principle by construction, also satisfies the Mermin-Wagner theorem: There is no finite-temperature phase transition breaking a continuous symmetry. Nevertheless, there is a crossover temperature below which the magnetic correlation length grows exponentially[28] until it reaches infinity at zero temperature. Detailed comparisons of the charge and spin structure factors, spin susceptibility, and double occupancy obtained with the TPSC scheme are in quantitative agreement with quantum Monte Carlo simulations for both nearest-neighbor[28,29] and next-nearest-neighbor[32] Hubbard models in two dimensions.

In loop expansions, response functions are computed at the one-loop level and self-energy effects appear only at the two-loop level. Similarly, in our case the second step of the approach gives a better approximation for the self-energy. We start from exact expressions for the self-energy with the fully reducible vertex expanded in either the longitudinal or the transverse channels. These exact expressions are easy to obtain within the functional derivative formalism. We insert in those expressions the TPSC results obtained at the first step, namely, U_{sp} and U_{ch}, $\chi_{sp}^{(1)}(q)$, $\chi_{ch}^{(1)}(q)$, and $G^{(1)}(k+q)$ so that Green functions, susceptibilities, and irreducible vertices entering the self-energy expression are all at the same level of approximation. Then considering both longitudinal and transverse channels, and imposing crossing symmetry of the fully reducible vertex in the two particle-hole channels, the final self-energy formula reads[33,31]

$$\Sigma_{\sigma}^{(2)}(k)=Un_{\bar{\sigma}}+\frac{U}{8}\frac{T}{N}\sum_{q}[3U_{sp}\chi_{sp}^{(1)}(q)+U_{ch}\chi_{ch}^{(1)}(q)]G_{\sigma}^{(1)}(k+q). \tag{8}$$

This self-energy (8) satisfies[28,31,33] the consistency condition between single- and two-particle properties, $\mathrm{Tr}(\Sigma^{(2)}G^{(1)})=2U\langle n_{\uparrow}n_{\downarrow}\rangle$. Internal consistency of the approach may be checked by verifying by how much $\mathrm{Tr}(\Sigma^{(2)}G^{(2)})$ differs from $2U\langle n_{\uparrow}n_{\downarrow}\rangle$. The results for single-particle properties given by the self-energy formula (8) are in quantitative agreement[28,33,34] with numerical simulations at weak to moderate couplings. At temperatures much lower than the crossover temperature where the correlation length increases exponentially, the consistency condition signals that the method becomes less accurate, although it does extrapolate in most cases to a physically reasonable zero-temperature limit.[28] In the present paper, we will not present results below the crossover temperature so we are always within the domain of validity. It should be noted that the self-energy Eq. (8) takes into account the fluctuations that are dominant already at the Hartree-Fock level, namely, the antiferromagnetic ones.

The above formalism can be extended[30] to compute pairing correlations. Physically, the $d_{x^2-y^2}$-wave susceptibility shows up after antiferromagnetic fluctuations have built up

since it is the latter that give some nontrivial momentum dependence to the vertices. Momentum dependence of the vertices is absent in the bare Hamiltonian and also at the first level of TPSC. It appears from the momentum dependence of the self-energy at the second level of approximation. In other words, our formalism physically reflects old ideas about pairing by antiferromagnetic spin waves.[35] What it contains that is absent in other formalisms is the possibility of suppression of superconductivity by pseudogap effects also induced by antiferromagnetic fluctuations.[30]

The mathematical procedure to obtain the $d_{x^2-y^2}$-wave pairing susceptibility is as follows. Basically, the above steps are repeated in the presence of an infinitesimal external pairing field that is eventually set to zero at the end of the calculation. This allows us to obtain the particle-particle irreducible vertex in Nambu space from the functional derivative of the off-diagonal $\Sigma^{(2)}$ with respect to the off-diagonal Green function. The d-wave susceptibility is defined by $\chi_d=\int_0^\beta d\tau\langle T_\tau\Delta(\tau)\Delta^\dagger\rangle$ with the $d_{x^2-y^2}$-wave order parameter $\Delta^\dagger=\Sigma_i\Sigma_\gamma g(\gamma)c_{i\uparrow}^\dagger c_{i+\gamma\downarrow}^\dagger$, the sum over γ being over nearest neighbors, with $g(\gamma)=\pm 1/2$ depending on whether γ is a neighbor on the $\hat{\mathbf{x}}$ or on the $\hat{\mathbf{y}}$ axis. $\beta\equiv 1/T$, T_τ is the time-ordering operator, and τ is imaginary time. The final expression for the $d_{x^2-y^2}$-wave susceptibility is

$$\begin{aligned}\chi_d(\mathbf{q}=0,\, iq_m=0) &= \frac{T}{N}\sum_k\,[g_d^2(\mathbf{k})G_\uparrow^{(2)}(-k)G_\downarrow^{(2)}(k)] \\ &- \frac{U}{4}\left(\frac{T}{N}\right)^2\sum_{k,k'}\,g_d(\mathbf{k})G_\uparrow^{(2)}(-k)G_\downarrow^{(2)}(k) \\ &\times\left(\frac{3}{1-\frac{U_{sp}}{2}\chi_0(k'-k)}+\frac{1}{1+\frac{U_{ch}}{2}\chi_0(k'-k)}\right) \\ &\times G_\uparrow^{(1)}(-k')G_\downarrow^{(1)}(k')g_d(\mathbf{k}'),\end{aligned} \tag{9}$$

with $g_d(\mathbf{k})=(\cos k_x-\cos k_y)$ being the form factor appropriate for d-wave symmetry. The above expression contains only the first two terms of the infinite series corresponding to the Bethe-Salpeter equation. It should be noted that the appearance of $G^{(2)}$ on the right-hand side of the equation for the susceptibility Eq. (9) allows pseudogap effects to suppress superconductivity.[30] This effect is absent in conventional treatments of pairing induced by antiferromagnons.

Since the crossover to the ferromagnetic ground state found in our work appears at very low temperatures ($T\leqslant 1/200$), a large lattice is required in order to avoid finite-size effects at those temperatures. In the case of ferromagnetism, sensitivity of the results to the lattice size at low T can be avoided by making sure that the lattice is large enough at any given temperature to reproduce the weak $\ln T$ behavior of the bare particle-hole susceptibility $\chi_0(\mathbf{q}=0,\, iq_m=0)$. That singularity reflects the singular density of states at the van Hove filling. We found that an $N=2048\times 2048$ lattice suffices to compute χ_0 entering the TPSC phase diagram. The sum over $\mathbf{q}$ in Eq. (4) can be performed on a coarser mesh without loss of precision. To speed up the calculations and to overcome increasing memory requirements, especially at low temperatures, we use the renormalization-group acceleration scheme.[36] Interpolation is used to obtain quantities at temperatures that fall between those directly obtained with the renormalization-group acceleration scheme.

III. WEAK FERROMAGNETISM AND OTHER INSTABILITIES

Without loss of generality, we can take $t>0$ and $t'\leqslant 0$. In that case, the van Hove filling is always at $n\leqslant 1$. The van Hove fillings $n\geqslant 1$ occur only when t and t' have the same sign, but this case can be mapped back to the situation $n\leqslant 1$ using the particle-hole transformation $c_{i\sigma}^\dagger\rightarrow(-1)^i d_{i\sigma}$ and $c_{i\sigma}\rightarrow(-1)^i d_{i\sigma}^\dagger$ where the phase factor takes the value $+1$ on one of the two sublattices of the bipartite lattice and -1 on the other sublattice. The sign of t and t' can be changed simultaneously with the particle-hole transformation defined by $c_{i\sigma}^\dagger\rightarrow d_{i\sigma}$ and $c_{i\sigma}\rightarrow d_{i\sigma}^\dagger$. Whenever a particle-hole transformation is performed, the occupation number changes from n to $2-n$. The van Hove filling vanishes at $|t'|=0.5|t|$ so we restrict ourselves to $|t'|<0.5|t|$. For larger $|t'|$ there is a change in Fermi surface topology.

We begin with the RPA phase diagram in the T-t' plane, then move to the TPSC crossover diagram and conclude with a short section on effects that can be detrimental to ferromagnetism.

A. RPA phase diagram

Within RPA or mean field, the transition temperature T_c may be found from

$$2-U\chi_0(\mathbf{q},0)=0, \tag{10}$$

where $\chi_0(\mathbf{q},0)$ is the zero-frequency limit of the noninteracting particle-hole susceptibility given by Eq. (6). In the case of ferromagnetism $\mathbf{q}=(0,0)$, while $\mathbf{q}=\mathbf{Q}\equiv(\pi,\pi)$ in the case of commensurate antiferromagnetism. The temperature at which the uniform paramagnetic phase becomes unstable to fluctuations at the antiferromagnetic (AFM) or at the ferromagnetic (FM) wave vector is plotted in Fig. 1. One should keep in mind that, in all cases, we are speaking of spin-density waves, namely, the local moment is in general smaller than the full moment. Furthermore, for $|t'|$ different from zero, the real wave vector where the instability occurs is incommensurate. The question of incommensurability is considered in more details in the TPSC section. Note that in contrast to the case $U=3$, the ferromagnetic critical temperature for $U=6$ does not increase with t', it even decreases slightly. We do not explore the stability of the various phases that could occur in mean-field theory below the indicated transition lines.

In both RPA and TPSC, the wave vector where the instability first develops is related to the $\mathbf{q}$ dependence of χ_0. In TPSC, it is not only the maximum value of $\chi_0(\mathbf{q},0)$ that determines the crossover temperature, but also the whole $\mathbf{q}$

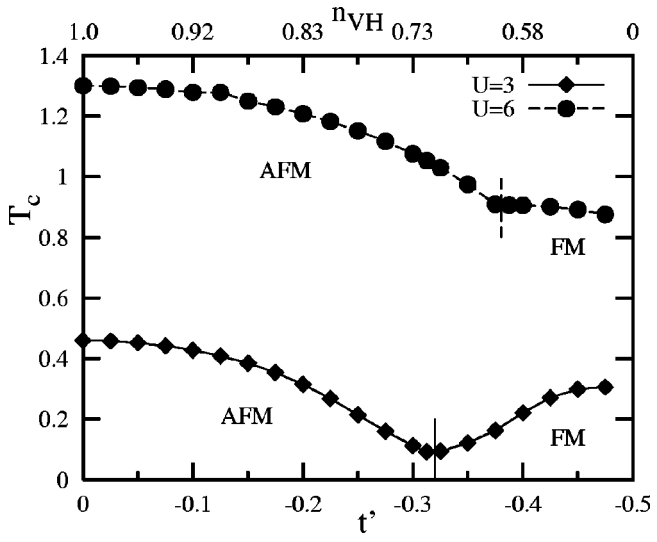

FIG. 1. The RPA critical temperature T_c as a function of the van Hove fillings indicated on the upper horizontal scale and the corresponding value of next-nearest-neighbor hopping t' on the lower horizontal scale. The critical temperature T_c is determined from Eq. (10). AFM stands for the region where the uniform paramagnetic phase becomes unstable to fluctuations at (π,π) while FM is the region where the instability is at (0,0). Vertical lines denote the boundary between AFM and ferromagnetic phases.

dependence of χ_0 that comes in the sum rule Eq. (4) for U_{sp}. From the plot of χ_0 as a function of wave vector at $T=0.01$ in Fig. 2, one can see that at $t'=0$ the antiferromagnetic wave vector $\mathbf{Q}$ leads to the largest value of χ_0. With increasing $|t'|$ the maximum of χ_0 is at an incommensurate wave vector $\mathbf{Q}_\delta=(\pi-\delta,\pi)$ close to (π,π), while for large $|t'|>0.32$ the maximum moves clearly to (0,0). For intermediate negative values of the next-nearest-neighbor hopping $|t'|\sim 0.3$ the magnitudes of the susceptibility at (0,0) and at (π,π) are comparable so the change in the relative magnitude as a function of temperature is important.

The main deficiencies of RPA are (a) finite-temperature phase transitions in two dimensions that contradict the Mermin-Wagner theorem, (b) an overestimation of the effect of U on T_c because of the neglect of the renormalization of U brought about by quantum fluctuations (Kanamori screening). One can see from Fig. 1 that the RPA critical temperature is quite a bit larger than the crossover lines predicted by the TCRG (see Fig. 1 of Ref. 19). The TPSC remedies these deficiencies.

B. TPSC crossover diagram

We begin by considering the effective interaction U_{sp} that plays a crucial role in TPSC. In Fig. 3 we plot U_{sp} as a function of t' as obtained from Eqs. (3)–(5). One can see that Kanamori screening strongly renormalizes the effective interactions. This weakly temperature dependent renormalization effect is stronger for large $|t'|$ in comparison with small $|t'|$. To explain this behavior we consider the sum rule that determines U_{sp}, Eq. (4). The main contribution to the sum on the left-hand side of this equation comes from the

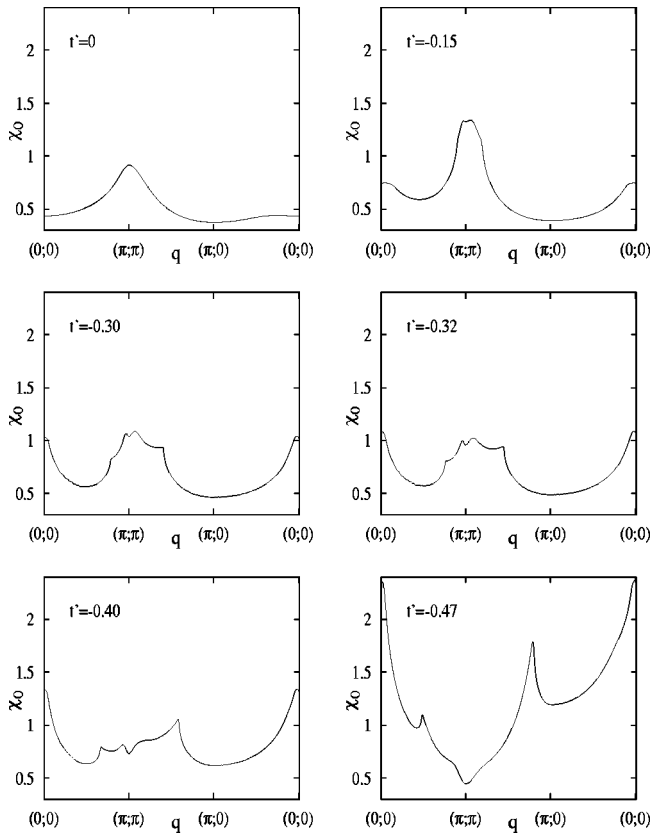

FIG. 2. The noninteracting particle-hole susceptibility χ_0 at zero frequency as a function of wave vector $\mathbf{q}$ along a path in the Brillouin zone is drawn for various values of next-nearest-neighbor hopping t' at $T=0.01$. The filling is obtained by placing the chemical potential at the energy of the van Hove singularity for the given t'.

small denominator caused, for large $|t'|$ by $\chi_0(\mathbf{0},0)$, and for small $|t'|$ by $\chi_0(\mathbf{Q},0)$. As the coefficient before the logarithm scales as $[\sqrt{1-4(t'/t)^2}]^{-1}$ for $\chi_0(\mathbf{0},0)$, and as $\ln([1+\sqrt{1-4(t'/t)^2}]/(2t'/t))$ for $\chi_0(\mathbf{Q},0)$, it turns out that $\chi_0(\mathbf{0},0)$ increases rapidly for $|t'|$ near 0.5. This means that U_{sp} has to decrease at large $|t'|$ to satisfy the sum rule (4) where, in addition, the quantity $n-2\langle n_\uparrow n_\downarrow\rangle$ on the right-hand side is a decreasing function of density (and hence of $|t'|$).

To find the crossover lines, we consider the zero-frequency limit of the spin susceptibility given by Eq. (5) and the $d_{x^2-y^2}$-wave pairing susceptibility given by Eq. (9) above. The crossover temperature T_X for the magnetic instabilities is chosen as the temperature where the enhancement factor $\chi_{sp}(\mathbf{q},0)/\chi_0(\mathbf{q},0)$ is equal to 500. We have checked that this corresponds to a magnetic correlation length that fluctuates around 25 lattice spacings for $|t'|$ between $|t'|=0$ and $|t'|=0.3$. The crossover temperature T_X is not very sensitive to the choice of criterion because near and below the crossover region the enhancement factor grows very rapidly (exponentially).

For pairing, we proceed as follows. Equation (9) contains only the first two terms of the infinite Bethe-Salpeter series. The first term (direct term) describes the propagation of dressed electrons that do not interact with each other while

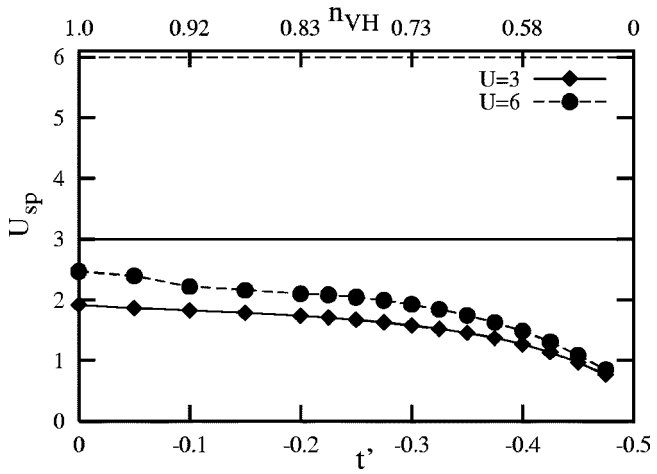

FIG. 3. Irreducible spin vertex U_{sp} as a function of next-nearest-neighbor hopping t' (or corresponding van Hove fillings on the upper horizontal scale) at $T=0.125$. Horizontal lines at $U=3,6$ denote the bare Hubbard repulsion U.

the second term contains one spin-fluctuation (and charge-fluctuation) exchange. This comes about in our formalism because $\Sigma^{(2)}$ is a functional of $G^{(1)}$. We would have obtained an infinite number of spin- and charge-fluctuation exchanges, in the usual Bethe-Salpeter way, if we could have written $\Sigma^{(2)}$ as a functional of $G^{(2)}$. This is not possible within TPSC. We have only the first two terms of the full series. The superconducting transition temperature in two dimensions is of the Kosterlitz-Thouless type and is expected to occur somewhat below the temperature determined from the Bethe-Salpeter equation (Thouless criterion). We thus use, as a rough estimate for the transition temperature for *d*-wave superconductivity, the temperature where the contribution of the vertex part (exchange of one spin and charge fluctuation) becomes equal to that of the direct part (first term) of the *d*-wave pairing susceptibility.[30] In other words, we look for the equality of the sign and the magnitude of the two terms appearing in Eq. (9). This choice is motivated by the statement that $1+x+\cdots$ resummed to $1/(1-x)$ diverges when $x=1$.

The TPSC phase diagram shows three distinct regions illustrated for $U=3$ and for $U=6$ in Fig. 4: (a) for $t'=0$, the leading instability is at the antiferromagnetic wave vector and for small nonvanishing $|t'|$ it is at an incommensurate wave vector close to (π,π). We will loosely refer to that region as the region where antiferromagnetism dominates. (b) For intermediate values of the next-nearest-neighbor hopping, $d_{x^2-y^2}$-wave superconductivity dominates. (c) At large negative $|t'|>0.33$ a crossover to a magnetic instability at the ferromagnetic wave vector occurs. Let us consider these different regions in turn.

Near $t'=0$, T_X is relatively high and the susceptibility near the antiferromagnetic wave vector grows most rapidly. When we increase $|t'|$, the crossover temperature decreases because of reduced nesting of the Fermi surface. In TPSC the wave vector of the instability is incommensurate for any finite value of the next-nearest-neighbor hopping $|t'|$ as can be concluded from the structure of Eq. (5) and from the fact that

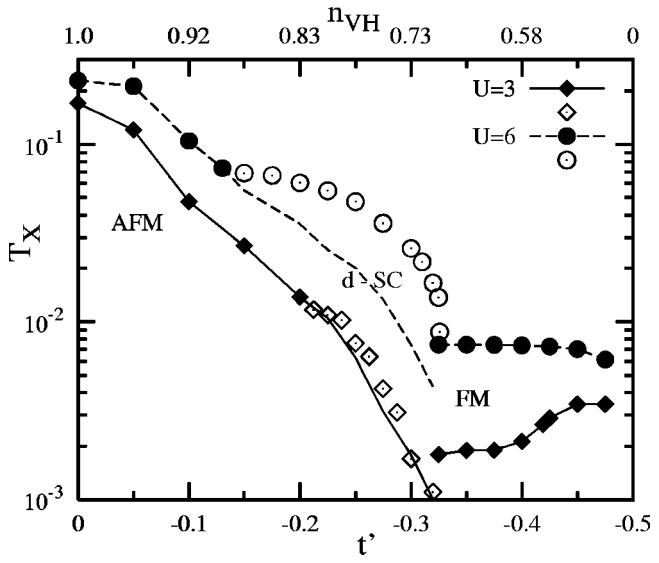

FIG. 4. The TPSC phase diagram as a function of next-nearest-neighbor hopping t' (lower horizontal axis). The corresponding van Hove filling is indicated on the upper horizontal axis. Crossover lines for magnetic instabilities near the antiferromagnetic and ferromagnetic wave vectors are represented by filled symbols while open symbols indicate instability towards $d_{x^2-y^2}$-wave superconducting. The solid and dashed lines below the empty symbols show, respectively, for $U=3$ and $U=6$, where the antiferromagnetic crossover temperature would have been in the absence of the superconducting instability. The largest system size used for this calculation is 2048×2048.

the noninteracting susceptibility with momenta $\mathbf{Q}_\delta=(\pi-\delta,\pi)$ is the largest when $t'\neq0$. The incommensurate wave vectors are plotted in Fig. 5 as a function of t'. One can see that the degree of incommensurability is strongly temperature dependent, and that it increases with increasing temperature.

In the second region of the TPSC phase diagram $d_{x^2-y^2}$-wave superconductivity is the leading instability. In

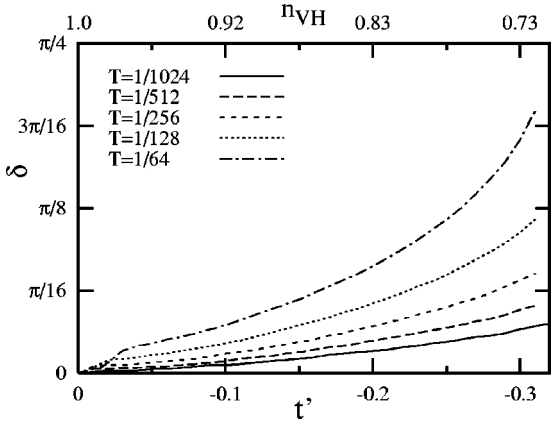

FIG. 5. Incommensurate wave vector $\mathbf{Q}_\delta=(\pi-\delta,\pi)$ where the maximum of the noninteracting susceptibility is located as a function of next-nearest-neighbor hopping t' at van Hove fillings. Different lines correspond to different temperatures. Given t' and a crossover temperature in the TPSC phase diagram, one can use the present figure to find out the incommensurate wave vector at which the instability first occurs.

this regime the transition temperature to $d_{x^2-y^2}$-wave superconductivity appears higher than the temperature at which the antiferromagnetic correlation length becomes larger than about 25. The latter crossover lines are denoted by the solid ($U=3$) and by the dashed lines ($U=6$) in Fig. 4. Note that $d_{x^2-y^2}$-wave superconductivity is here induced by incommensurate antiferromagnetic fluctuations. While high-temperature superconductors are not generally close to van Hove singularities, incommensurate dynamic spin fluctuations are concomitant with $d_{x^2-y^2}$ superconductivity in these compounds.[37]

Finally, the third regime occurs at $|t'|>0.33$ where the ferromagnetic susceptibility $\chi_{sp}(\mathbf{0},0)$ is the leading one at low temperatures. Ferromagnetism occurs because of the diverging density of states at the van Hove singularity.

Note that for U infinitesimally small the phase boundaries happen close to zero temperature. Disregarding superconductivity for the moment, let us consider where the phase boundary between antiferromagnetism and ferromagnetism would be at small U. In that case, the asymptotic behavior of the Lindhard function near $\mathbf{q}=0$ and $\mathbf{q}=\mathbf{Q}$ is, respectively,[21]

$$\chi_0(\mathbf{0},0)\sim \ln[1/\max(\mu,T)]/\sqrt{1-R^2},$$

$$\chi_0(\mathbf{Q},0)\sim \ln[1/\max(\mu,T)]\ln[(1+\sqrt{1-R^2})/R],$$

with $R\equiv 2t'/t$ so that, looking at the equality of the coefficients of the logarithms, one finds that the change from antiferromagnetic to ferromagnetic behavior occurs at $|t'|=0.27$ instead of $|t'|=0.33$ as found above.[24,38] To understand the difference between these two results, we need to look at subdominant corrections. For example, a numerical fit reveals that $\chi_0(\mathbf{Q},0)\simeq 0.52+0.24\log_{10}(1/T)$. This means that for the leading term with a logarithmic structure to be, say, about ten times larger than the subdominant term, the temperature should be as low as 10^{-20}. The corresponding U (or U_{sp}) that satisfies $1=U$ (or $U_{sp})\chi_0(\mathbf{Q},0)/2$ at this temperature is very small, namely, $0.4t$. Therefore, unless U is very small, the next leading term plays an important role and a straightforward application of the asymptotic form (taking only the leading term) is not justified. For $U=6$ and $U=3$, for example, TPSC shows that near the antiferromagnetic to ferromagnetic boundary, the crossover temperature is of order 10^{-2} and 10^{-3}, respectively. For this temperature, the subleading term 0.52 is comparable to the logarithmic contribution.

The TPSC phase diagram is in qualitative agreement with the TCRG phase diagram.[19] In addition, the critical values t'_c for the stability of superconductivity and ferromagnetism are the same in both approaches. But in contrast with the TCRG, ferromagnetism in TPSC occurs at very low temperatures, and increasing $|t'|$ does not lead to a dramatic increase in crossover temperature. One can see from Fig. 4 that the critical values of t' for the stability of ferromagnetism are unchanged for different U, whereas the critical $|t'_c|$ for the stability of $d_{x^2-y^2}$-wave superconductivity decreases with increasing coupling strength U.

The fact that the crossover temperature towards ferromagnetism depends even more weakly on t' in TPSC than in RPA can be explained by the following simple argument. Taking into account Kanamori's improvement[3] of the naive Stoner criterion for ferromagnetism, we expect that the crossover temperature T_X can be roughly approximated by

$$T_X\sim T_0\exp\left(-\frac{1}{\rho(E_F)U_{\text{eff}}}\right), \tag{11}$$

where T_0 is a constant, $\rho(E_F)=\chi_0(\mathbf{0},0)/2$, and U_{eff} is the renormalized effective interaction (U_{sp} in the case of TPSC). We have already explained in the context of Fig. 3 that the increase with $|t'|$ of the weight of the logarithmic singularity in the density of states at the Fermi level leads to a decrease of U_{sp}, so the crossover temperature is almost constant in TPSC.

A distinctive feature of the TPSC phase diagram is that the crossover to ferromagnetism generally occurs at a much lower temperature than the crossover to antiferromagnetism. This partially comes from the peculiarity of the temperature dependence of the zero-frequency limit of the noninteracting particle-hole susceptibility. To demonstrate this, let us use, as an estimate for the crossover temperatures in TPSC, the RPA criterion Eq. (10) with U replaced by U_{sp} and let us look for values of the temperature when the left-hand side of that equation becomes small (it will vanish only at zero temperature). At small $|t'|$ the leading noninteracting staggered susceptibility $\chi_0(\mathbf{Q},0)$ behaves like $(\ln T)^2$ with temperature, while for $|t'|>0.33$ the leading noninteracting uniform susceptibility $\chi_0(\mathbf{0},0)$ scales as $|\ln T|$. We find that these susceptibilities have comparable size for temperatures $T\gtrsim 1$, while the divergences of $\chi_0(\mathbf{Q},0)$ and $\chi_0(\mathbf{0},0)$ begin, respectively, at $T<1$ and $T\ll 1$. Therefore, since the Stoner criterion Eq. (10) is satisfied in RPA with bare $U=3,6$ at temperatures $T\gtrsim 1$, RPA shows the same temperature scale for ferromagnetism and antiferromagnetism. But in TPSC the strong renormalization of the interaction strength $U_{sp}<U$ means that the crossover occurs for larger values of $\chi_0(\mathbf{Q},0)$ and $\chi_0(\mathbf{0},0)$, in a regime where they already have different scales since $\chi_0(\mathbf{Q},0)$ for small $|t'|$ starts to grow logarithmically at much higher temperature than $\chi_0(\mathbf{0},0)$ for large $|t'|$. Thus, the crossover to antiferromagnetism in TPSC occurs at much higher temperatures than the crossover to ferromagnetism.

Another interesting feature of the TPSC phase diagram at $U=3$ is that the crossover temperature for antiferromagnetism is of the same order of magnitude as that of the TCRG result of Ref. 19, whereas the crossover to ferromagnetism is at a much lower temperature than that observed in the TCRG calculations. The naive explanation is as follows. Let us assume that the approximate mean-field-like expression Eq. (11) for T_X has meaning both within TPSC and within TCRG except that U_{eff} has a different value in both approaches. Simple algebra then shows that the relation between the crossover temperatures for TPSC and TCRG in the ferromagnetically fluctuating regime is

$$\frac{T_{\text{FM}}^{\text{TCRG}}}{T_{\text{FM}}^{\text{TPSC}}}=\left(\frac{T_0}{T_{\text{FM}}^{\text{TPSC}}}\right)^{1-1/a},$$

with $a = U_{\mathrm{eff}}^{\mathrm{TCRG}}/U_{sp}$ characterizing the different renormalizations of U in both approaches. When $a=1$, both crossover temperatures are equal. For $a>1$ the TCRG value for T_X is larger than for TPSC while the reverse is true when $a<1$. Using the numerical result[39] for the TCRG effective interaction at $U=3$ and $|t'|\sim 0.45$ we have $a=1.4$–1.8. Then, replacing T_0 by the bandwidth $8t$ and taking $T_{\mathrm{FM}}^{\mathrm{TPSC}}=3.4\times 10^{-3}$ corresponding to $|t'|\geqslant 0.42$ we obtain the estimate $T_{\mathrm{FM}}^{\mathrm{TCRG}}/T_{\mathrm{FM}}^{\mathrm{TPSC}}\approx 10$–$30$. This agrees with the crossover temperatures extracted from the TPSC (Fig. 4) and the TCRG phase diagrams (Fig. 1 of Ref. 19). Similarly in the antiferromagnetically fluctuating regime near $|t'|=0$, we use the improved mean-field estimate for T_X,

$$T_X \sim T_0 \exp(-\sqrt{8t/U_{\mathrm{eff}}}),$$

to extract the following relation between the crossover temperatures:

$$\frac{T_{\mathrm{AFM}}^{\mathrm{TCRG}}}{T_{\mathrm{AFM}}^{\mathrm{TPSC}}} = \left(\frac{T_0}{T_{\mathrm{AFM}}^{\mathrm{TPSC}}}\right)^{1-1/\sqrt{a}}.$$

Using the value of U_{sp} from the TPSC and the TCRG effective interaction[39] at $U=3$ and $|t'|\sim 0.1$ we have $a=1.0$–1.4. This leads to $T_{\mathrm{AFM}}^{\mathrm{TCRG}}/T_{\mathrm{AFM}}^{\mathrm{TPSC}}\approx 1$–$2.5$ for $T_{\mathrm{AFM}}^{\mathrm{TPSC}}\sim 4\times 10^{-2}$ at $|t'|\sim 0.1$, which is in good agreement with the data extracted from the phase diagrams.

As mentioned at the beginning of this section, the crossover temperatures T_X for the magnetic instabilities in TPSC have been chosen such that the enhancement factor is equal to 500. The enhancement factor scales like the square of the correlation length ξ^2. For such large ξ^2 the value of T_X is rather insensitive to the choice 500 since the correlation length grows exponentially. Our criterion for T_X leads to a good estimate of the real phase-transition temperature with $\xi=\infty$ when a very small coupling term is added in the third spatial direction. The dependence of T_c on coupling in the third dimension has been studied, within TPSC, in Ref. 40. The latter reference also contains expressions for the relation between the enhancement factor and ξ^2. On the other hand, T_X depends more strongly on the precise criterion if we choose a moderate value of the enhancement factor. In particular, the TPSC value of T_X in the antiferromagnetic fluctuation region increases by a factor 2–5 if we choose 10 for the enhancement factor, close to the value[41] chosen in Ref. 19. In this case, T_X agrees essentially perfectly with the value obtained in the TCRG phase diagram.

Note however that our estimate for the superconducting transition temperature is smaller than that obtained with the TCRG of Ref. 19. Because in TPSC the pairing fluctuations do not feed back in the antiferromagnetic fluctuations, this result suggests that the feedback, usually included in TCRG, enhances superconductivity in this region of the phase diagram. Such a positive feedback effect was also found in the RG calculations of Refs. 42 and 17. On the other hand, the RG approach of Ref. 24 suggests instead that antiferromagnetism and superconductivity oppose each other. Some particle-particle diagrams were however neglected in the latter approach. In TPSC, antiferromagnetic fluctuations help $d_{x^2-y^2}$-wave superconductivity as long as they are not strong enough to create a pseudogap, in which case they are detrimental to superconductivity.[30]

The above-mentioned renormalization-group calculations were done in the one-loop approximation without self-energy effects. By contrast, in the RG work of Ref. 43, self-energy effects showing up at two loops were included in the calculation for the $t'=0$ model. There it was found that dressing the flow equations for AFM and superconducting response functions with the one-particle wave-vector-dependent weight factors Z results in a reduction of both AFM and superconducting correlations, the latter suppression being more pronounced. Within TPSC, the momentum- and frequency-dependent self-energy effects that appear in $G^{(2)}$ in the pairing susceptibility Eq. (9) do tend to decrease the tendency to pairing when AFM fluctuations become very strong at and near half-filling,[30] in qualitative agreement with the RG result.[43] In particular, in the presence of an AFM-induced pseudogap, the tendency to superconductivity is decreased compared to what it would be if we replaced $G^{(2)}$ by $G^{(1)}$ everywhere. (Such a replacement is not allowed within our formalism). Because of the excellent agreement between TPSC at the first level of approximation and quantum Monte Carlo calculations,[28,29] momentum- and frequency-dependent self-energy effects are not expected to be very important for AFM fluctuations unless we are deep in the pseudogap regime. They have not been taken into account at this point. They might be more important in the case of ferromagnetism, which is already a very weak effect in TPSC. This is discussed below.

C. Additional effects that may be detrimental to ferromagnetism

The TCRG phase diagram[19] is computed at the one-loop level. Self-energy effects occur at the two-loop level. Similarly, self-energy effects in TPSC are calculated at the second level of approximation. Since analytical continuation of imaginary-time results is difficult at low temperature, we estimate the quasiparticle weight with the help of the quantity $z'(T)$ defined in Refs. 28 and 44 by

$$z'(T) = -2G(\mathbf{k}_F, \beta/2) = \int \frac{d\omega}{2\pi} \frac{A(\mathbf{k}_F,\omega)}{\cosh(\beta\omega/2)}. \qquad (12)$$

Physically, this quantity is an average of the single-particle spectral weight $A(\mathbf{k}_F,\omega)$ within T of the Fermi level ($\omega=0$). When quasiparticles exist, this is a good estimate of the usual zero-temperature quasiparticle renormalization factor $z \equiv (1-\partial\Sigma/\partial\omega)^{-1}$. However, in contrast to the usual z, this quantity gives an estimate of the spectral weight $A(\mathbf{k}_F,\omega)$ around the Fermi level, even if quasiparticles disappear and a pseudogap forms.

Figure 6 shows the quasiparticle renormalization factor z' at a value $|t'|=0.4$ where ferromagnetic fluctuations dominate at very low temperatures. One observes a progressive decrease of $z'(T)$ with decreasing temperature. We checked that the single-particle spectral function $A(\mathbf{k}_F,\omega)$ begins to show a small *pseudogap* at the temperature where z' begins to decrease significantly. Since the ferromagnetic fluctuations

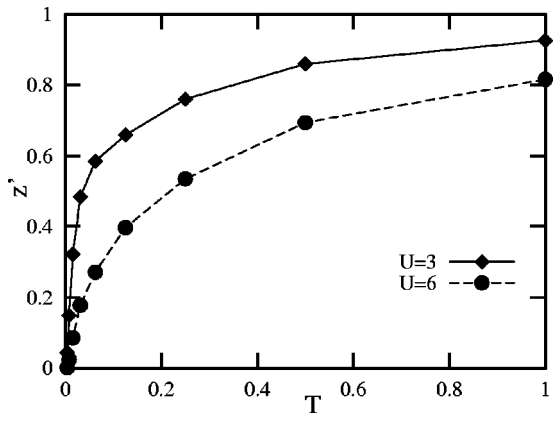

FIG. 6. Temperature dependence of $z'(T)$ defined by Eq. (12) at the van Hove filling corresponding to $|t'|=0.4$.

are not yet strong enough at that temperature to create a pseudogap, this effect is completely driven by the singular density of states at the van Hove filling. In other words, second-order perturbation theory should suffice to observe the effect. The analogous feature was previously found by one of the authors and his co-workers[45] in a second-order perturbation study of the nearest-neighbor two-dimensional Hubbard model at half-filling. Self-energy effects near van Hove points have also been discussed in Ref. 46. The rather strong suppression of spectral weight at the Fermi wave vectors for temperatures larger than the crossover temperature found in the above section would probably reduce the true T_X or even completely eliminate the possibility of a ferromagnetic ground state if we could include the feedback of this self-energy effect into the spin susceptibility.

The ferromagnetic fluctuation regime is also very sensitive to doping within TPSC. In fact, deviations of the filling by 2–3% away from the van Hove filling remove the crossover to the ferromagnetic regime.

There is also an argument that suggests that a Stoner-type ferromagnetic ground state is unstable in the two-dimensional Hubbard model. Within RPA in the ferromagnetic state,[47] the spin stiffness constant for spin waves in the ferromagnetic state is proportional to minus the second derivative of the density of states at the Fermi level.[48] Since the density of states as a function of energy (away from the van Hove filling) has a positive curvature in two dimensions, it leads to a negative spin stiffness constant and thus to an instability. This argument is based on the noninteracting density of states. The pseudogap effect mentioned above changes the curvature of the density of states at the Fermi level and may stabilize the ferromagnetic state.

IV. CONCLUSIONS

As found within temperature-cutoff renormalization group (TCRG),[19,27] TPSC suggests that ferromagnetism may appear in the phase diagram of the 2D t-t' Hubbard model at van Hove fillings for weak to intermediate coupling. It is striking that the overall phase diagrams of TCRG and TPSC have some close similarities. As in TCRG, we find, Fig. 4, that for small negative values of the next-nearest-neighbor hopping the leading instability is a spin-density wave with slightly incommensurate antiferromagnetic wave vector (Fig. 5). We could find incommensurability at small $|t'|$ only for very large lattice sizes. The TCRG seems to indicate that very close to $|t'|=0$, the wave vector remains pinned at (π,π) (Ref. 27) but that could be due to the fact that coupling constants in TCRG represent a finite region in wave-vector space and hence very small incommensurabilities cannot be resolved. For intermediate values of $|t'|$ we also find $d_{x^2-y^2}$-wave superconductivity. The precise value of $|t'|$ for the onset of $d_{x^2-y^2}$-wave superconductivity depends somewhat on the criterion used for the crossover temperature. One clear difference with TCRG, however, is that the range of $|t'|$ where superconductivity appears increases with U whereas it decreases with U in TCRG.[27] At large $|t'|>0.33t$, a crossover to ferromagnetism occurs as a result of the diverging density of states. TPSC cannot tell us what happens below the crossover temperature, but that temperature is the relevant one in practice since any small coupling in the perpendicular direction would lead to a real phase transition.

The critical value for ferromagnetism, $|t'|=0.33t$, coincides with that found in TCRG.[19,27] This value of $|t'|$ is smaller than that found within the T-matrix approximation,[21] but that may be because of the cutoff to the van Hove singularity imposed by the small system sizes used in that approach. The critical value for ferromagnetism, $|t'|=0.33t$, also differs from the value $|t'|=0.27t$ obtained in Ref. 24 in the limit of zero temperature. We have explained in Sec. III B that for the crossover to occur sufficiently close to $T=0$ for the arguments of Ref. 24 to be correct, one needs values of U that are unrealistically small. At finite U (we studied $U=3$ and $U=6$), subdominant corrections to the logarithms shift the critical $|t'/t|=0.27$ found in Ref. 24 to the value $|t'/t|=0.33$ found by us and TCRG.

The differences between TCRG and other approaches, as well as their strengths and weaknesses, are well explained in Refs. 19 and 27. The smaller temperature scale for crossover to $d_{x^2-y^2}$-wave superconductivity in TPSC is a difference worth noting between our approach and TCRG.[19] This may be due to the fact that our calculations include self-energy effects which are absent[43] in one-loop TCRG. But the most striking difference is the temperature scale for ferromagnetism that in our case remains extremely small away from the critical $|t'|=0.33t$.

We have shown that the low-temperature scale for the crossover to ferromagnetic fluctuations comes from Kanamori screening that strongly renormalizes the effective interaction (this effect is smaller in the antiferromagnetic regime). In TPSC this renormalization comes from the constraint that the spin response function with U_{sp} should satisfy the local moment sum rule, Eq. (4). This causes the crossover temperature to ferromagnetic fluctuations to depend weakly on t' and to remain small. As in the T-matrix approximation,[21] Kanamori screening seems much stronger than what is obtained with TCRG. The latter approach perhaps does not include all the large wave vectors and large energies entering the screening of the effective interaction.

Within TPSC then, the tendency to ferromagnetism seems

very fragile. In addition, we checked that in TPSC ferromagnetism disappears for electron concentrations that are only very slightly (2–3%) away from van Hove fillings, in overall agreement with the results of the TCRG.[19,27] So the question of the existence of Stoner-type ferromagnetism at weak to intermediate coupling is not completely settled yet, despite the positive signs and the concordance of the most reliable approaches. We have estimated the electronic self-energy effects for large $|t'|$ and found that the quasiparticle renormalization factor is reduced significantly at temperatures $T<0.1$. As a result, the single-particle spectral function $A(\mathbf{k}_F,\omega)$ starts to show a small pseudogap which, at high temperature, is completely driven by the singular density of states, and not by the ferromagnetic fluctuations that appear only at very low temperature. This rather strong suppression of spectral weight at the Fermi wave vectors for $T>T_X$ may further reduce T_X or even completely eliminate the crossover to a ferromagnetic ground state. We have argued in Sec. III C that other factors could be detrimental to a ferromagnetic ground state in two dimensions. In particular, as is the case with RG calculations,[19,27] a consistent treatment of the electronic self-energy effects on the spin response function remains an open issue.

Another interesting problem for future investigations is the question of whether ferromagnetism could compete with the Pomeranchuk instability, i.e., a spontaneous deformation of the Fermi surface reducing its symmetry from the tetragonal to the orthorhombic one. Temperature cutoff RG (Refs. 27,49) disagrees with a suggestion[16,20,50] that this is one of the possible leading instabilities of the 2D t-t' Hubbard model at van Hove fillings.

Note added in proof: B. Binz, D. Baeriswyl, and B. Douçot [Ann. Phys. (Leipzig) **12** (2003); cond-mat/0309645] have recently questioned the application of one-loop renormalization group to ferromagnetism, suggesting that the error produced by the one-loop approximation is of the same order as the term which produces the ferromagnetic instability.

ACKNOWLEDGMENTS

We are particularly indebted to A. Katanin for sharing his unpublished data with us and for numerous useful discussions. The authors also thank M. Salmhofer, C. Honerkamp, C. Bourbonnais, M. Azzouz, and M. Gingras for valuable discussions. The present work was supported by the Natural Sciences and Engineering Research Council (NSERC) of Canada, the Fonds Québécois de la recherche sur la nature et les technologies, the Canadian Foundation for Innovation and the Tier I Canada Research Chair Program (A.-M.S.T.).

[1] M.C. Gutzwiller, Phys. Rev. Lett. **10**, 59 (1963).
[2] J. Hubbard, Proc. R. Soc. London, Ser. A **276**, 238 (1963).
[3] J. Kanamori, Prog. Theor. Phys. **30**, 275 (1963).
[4] For a review see, P. Fazekas, *Lecture Notes on Electron Correlation and Magnetism* (World Scientific, Singapore, 1999).
[5] Y. Nagaoka, Phys. Rev. **147**, 392 (1966).
[6] D.J. Thouless, Proc. Phys. Soc. London **86**, 893 (1965).
[7] T. Hanisch, G.S. Uhrig, and E. Müller-Hartmann, Phys. Rev. B **56**, 13 960 (1997).
[8] E.H. Lieb, Phys. Rev. Lett. **62**, 1201 (1989).
[9] A. Mielke and H. Tasaki, Commun. Math. Phys. **158**, 341 (1993).
[10] H. Tasaki, Prog. Theor. Phys. **99**, 489 (1998).
[11] A. Mielke, Phys. Rev. Lett. **82**, 4312 (1999).
[12] H. Tasaki, cond-mat/0301071, Commun. Math. Phys. (to be published 2003).
[13] D. Vollhardt, N. Blümer, K. Held, M. Kollar, J. Schlipf, M. Ulmke, and J. Wahle, Adv. Solid State Phys. **35**, 383 (1999).
[14] L. Chen, C. Bourbonnais, T. Li, and A.-M.S. Tremblay, Phys. Rev. Lett. **66**, 369 (1991).
[15] W. Hofstetter and D. Vollhardt, Ann. Phys. (Leipzig) **7**, 48 (1998).
[16] C. Halboth and W. Metzner, Phys. Rev. Lett. **85**, 5162 (2000); Phys. Rev. B **61**, 7364 (2000).
[17] C. Honerkamp, M. Salmhofer, N. Furukawa, and T.M. Rice, Phys. Rev. B **63**, 035109 (2001).
[18] H.Q. Lin and J.E. Hirsch, Phys. Rev. B **35**, 3359 (1987).
[19] C. Honerkamp and M. Salmhofer, Phys. Rev. Lett. **87**, 187004 (2001); Phys. Rev. B **64**, 184516 (2001).
[20] V. Hankevych, I. Grote, and F. Wegner, Phys. Rev. B **66**, 094516 (2002); V. Hankevych and F. Wegner, Eur. Phys. J. B **31**, 333 (2003).
[21] R. Hlubina, S. Sorella, and F. Guinea, Phys. Rev. Lett. **78**, 1343 (1997); R. Hlubina, Phys. Rev. B **59**, 9600 (1999).
[22] M. Fleck, A.M. Oleś, and L. Hedin, Phys. Rev. B **56**, 3159 (1997).
[23] L. Arrachea, Phys. Rev. B **62**, 10 033 (2000). These exact diagonalizations were done on larger lattices than those in Ref. 18 which did not find a ferromagnetic solution, in contradiction with this more recent work. The recent work also considered a wider range of boundary conditions.
[24] J.V. Alvarez, J. González, F. Guinea, and A.H. Vozmediano, J. Phys. Soc. Jpn. **67**, 1868 (1998).
[25] V.Yu. Irkhin, A.A. Katanin, and M.I. Katsnelson, Phys. Rev. B **64**, 165107 (2001).
[26] C. Bourbonnais, Ph.D. thesis, Université de Sherbrooke, 1985 (unpublished); C. Bourbonnais, Mol. Cryst. Liq. Cryst. **119**, 11 (1985); L.G. Caron and C. Bourbonnais, *ibid.* **119**, 451 (1985); C. Bourbonnais and L.G. Caron, Int. J. Mod. Phys. B **5**, 1033 (1991); H. Nélisse, C. Bourbonnais, H. Touchette, Y.M. Vilk, and A.-M.S. Tremblay, Eur. Phys. J. B **12**, 351 (1999).
[27] A.A. Katanin and A.P. Kampf, cond-mat/0304189 (unpublished).
[28] Y.M. Vilk and A.-M.S. Tremblay, J. Phys. I **7**, 1309 (1997).
[29] Y.M. Vilk, L. Chen, and A.-M.S. Tremblay, Phys. Rev. B **49**, 13 267 (1994).
[30] B. Kyung, J.-S. Landry, and A.-M.S. Tremblay, Phys. Rev. B **68**, 174502 (2003); B. Kyung, S. Allen, and A.-M. S. Tremblay (unpublished).
[31] S. Allen, A.-M. S. Tremblay, and Y. M. Vilk, in *Theoretical Methods for Strongly Correlated Electrons*, edited by David Sénéchal, André-Marie Tremblay, and Claude Bourbonnais,

CRM Series in Mathematical Physics (Springer, New York, 2003).
[32] A.F. Veilleux, A.-M. Daré, L. Chen, Y.M. Vilk, and A.-M.S. Tremblay, Phys. Rev. B **52**, 16 255 (1995).
[33] S. Moukouri, S. Allen, F. Lemay, B. Kyung, D. Poulin, Y.M. Vilk, and A.-M.S. Tremblay, Phys. Rev. B **61**, 7887 (2000).
[34] B. Kyung, J.S. Landry, D. Poulin, and A.-M.S. Tremblay, Phys. Rev. Lett. **90**, 099702 (2003).
[35] D.J. Scalapino, Phys. Rep. **250**, 329 (1995).
[36] C.-H. Pao and N.E. Bickers, Phys. Rev. B **49**, 1586 (1994).
[37] K. Yamada, C.H. Lee, K. Kurahashi, J. Wada, S. Wakimoto, S. Ueki, H. Kimura, Y. Endoh, S. Hosoya, G. Shirane, R.J. Birgeneau, M. Greven, M.A. Kastner, and Y.J. Kim, Phys. Rev. B **57**, 6165 (1998).
[38] We thank A. Katanin for pointing this out to us.
[39] A.A. Katanin (private communication).
[40] A.-M. Daré, Y.M. Vilk, and A.-M.S. Tremblay, Phys. Rev. B **53**, 14 236 (1996).
[41] In the RG phase diagram of Ref. 19 T_X is defined as the temperature where the coupling constant reaches $18t$, which corresponds to the enhancement factor of ≈ 20. C. Honerkamp (private communication).
[42] C. Bourbonnais and R. Duprat, Eur. Phys. J. B **21**, 219 (2001).
[43] D. Zanchi, Europhys. Lett. **55**, 376 (2001).
[44] Y.M. Vilk and A.-M.S. Tremblay, Europhys. Lett. **33**, 159 (1996).
[45] F. Lemay, Y. M. Vilk, and A.-M. S. Tremblay (unpublished); F. Lemay, Ph.D. thesis, Université de Sherbrooke, 2000 (unpublished).
[46] V.Yu. Irkhin and A.A. Katanin, Phys. Rev. B **64**, 205105 (2001); Erratum, cond-mat/0105564 (unpublished); cond-mat/0310112 (unpublished).
[47] S. Doniach and E.H. Sondheimer, *Green's Functions for Solid State Physicists* (Imperial College Press, London, 1998).
[48] P. Nozières (unpublished).
[49] C. Honerkamp, M. Salmhofer, and T.M. Rice, Eur. Phys. J. B **27**, 127 (2002).
[50] A. Neumayr and W. Metzner, Phys. Rev. B **67**, 035112 (2003).